Selective control of quantum Hall edge-channel trajectories by scanning gate microscopy

Electronic Mach–Zehnder interferometers in the quantum Hall regime are currently discussed for the realization of quantum information schemes. A recently proposed device architecture employs interference between two co-propagating edge channels (see the report of V. Giovannetti). Here we demonstrate the precise control of individual edge-channel trajectories in quantum point contact devices in the quantum Hall regime. The biased tip of an atomic force microscope is used as a moveable local gate to pilot individual edge channels. Our results are discussed in light of the implementation of multi-edge interferometers.

Stefan Heun

stefan.heun@sns.it

Collaborators
F. Beltram
G. Biasiol
N. Paradiso
L.N. Pfeiffer
S. Roddaro
L. Sorba
K.W. West

Interference phenomena are a fundamental manifestation of the quantum mechanical nature of electrons and have promising applications in solid-state quantum information technology. Two-dimensional electron systems (2DES) in the quantum Hall (QH) regime are especially suited for this purpose given the large electronic coherence length characteristic of edge-channel chiral transport. In particular, the realization of electronic Mach–Zehnder (MZ) interferometers in QH systems appears at present a sound technology for the implementation of quantum information schemes [1]. Despite this success, the edge topology of the single-channel MZ limits the complexity of these circuits to a maximum of two interferometers [2]. In order to overcome this constraint, new device architectures were recently proposed [3], where interference paths are built using two different parallel edge channels. In this configuration, control over the interaction between the different edge channels is challenging owing to the complexity of the edge structure. In order to address these issues we are exploring the use of scanning gate microscopy (SGM) to control the trajectory and interaction of edge channels based on our previous results on quantum point contact (QPC) devices in the QH regime [4–7]. In the present work, the two split gates of the QPC play a double role: they not only allow us to bring the edges in close proximity, but they also provide the ability to select the edges that are sent to the center of the QPC.

Experiments were performed in the new SGM laboratory at NEST (Fig. 1a). The activity is aimed at combining our experience with transport properties of nanostructures with the opportunity of investigation offered by scanning probe microscopy operating at ultra-low temperature (300mK), in a magnetic field tunable up to 9T. The recently installed instrument allows to locally apply an electric potential by means of the conductive tip of an atomic force microscope (AFM) operating in non-contact mode. The

Fig. 1
(a) The new SGM lab at NEST. (b) The AFM head for SGM measurements.

fundamental element of our SGM system is the AFM head (Fig. 1b). The upper part contains the sample holder with the wires for transport measurements. This is placed on a stack of piezo actuators providing the coarse and fine positioning of the sample, which allow sample movements of several millimeters with a sub-micron resolution and reproducibility. The lower part of the AFM head contains the tuning fork with the conductive tip, which allows us to both measure the sample topography and to apply a local potential. Our setup is also equipped with a STM head, which is capable of obtaining topographic images of conductive samples with atomic resolution. Both the AFM and the STM heads are non-magnetic (all the metallic parts are in titanium) and are designed to suitably work either at ultralow temperature or at room temperature. They are mounted to the cold finger of a 3He cryostat. The cryostat is inserted in a dewar suspended by means of springs in a soundproofed box in order to damp mechanical and acoustical noise. For low temperature operations a magnetic field up to 9 T is provided by a superconducting coil placed at the bottom of the dewar.

In order to validate our microscope setup we performed SGM measurements on QPCs at zero magnetic field. When the QPC conductance is quantized, the depletion spot induced by the tip causes a backscattering of electrons through the QPC [8,9]. When the tip is located above areas with high electron flow, the conductance is reduced by this effect, while it remains constant over areas with small electron flow. Scanning the tip over the sample yields therefore images of electron flow. The conductance map in Fig. 2 shows the characteristic branched flow of electrons. These branches correspond to the paths of lowest energy for the electrons moving in the potential landscape of the 2DES. They extend over a length scale of about 5μm due to the high mobility of the 2DES. The fringes decorating these structures are separated by half the Fermi wavelength. This can be better seen in the inset of Fig. 2 which shows a high-resolution image of one of the branches. The fringes are clearly resolved. They are due to the interference between time-reversed electron paths from the QPC and from the depletion spot generated by the AFM tip.

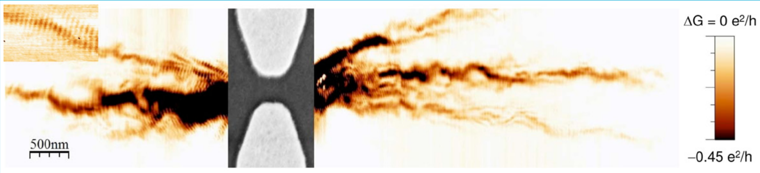

Fig. 2
Characteristic branched flow observed in zero-field SGM measurements. The image shows the change in conductance ΔG as a function of tip position. The dark regions in the color plot (low conductance) correspond to the actual electron path and depend on the details of the local potential. The center part of the image shows a scanning electron microscopy image of the QPC. Inset: The fringes which decorate the branches are a signature of the electron phase coherence.

The present work is aimed at exploring the use of SGM to control the trajectory and the interaction of edge channels in the QH regime. The fundamental idea behind our experiments consists in exploiting the QPC not only to control the distance between counterpropagating edges (as in tunnelling experiments [6,7]) but also to set the number of edges flowing around each of the two split gates. An essential role here is played by the SGM tip, which is exploited first to determine the filling factor underneath the two split gates and then to put the selected edge states in interaction. All the experiments discussed in the following were performed at bulk 2DES filling factor $\nu = 4$. Since at this magnetic field the Zeeman splitting is too small to be observed in our experiment, we are studying two spin-degenerate edge channels here.

Fig. 3 shows the QPC conductance as a function of the position of the biased SGM tip. In the panel (a) the gate-region filling factors are g1 = g2 = 0. When the biased tip is brought close to the QPC, pairs of edge channels are backscattered one by one, and the conductance through the

QPC decreases in a step-like manner to 0. This clearly demonstrates the gating action of the tip even in the QH regime. Taking advantage of the high flexibility of our setup, we repeated the SGM measurements also in asymmetric configurations such as that shown in the panel (b) of Fig. 3, where $g_1 = 0$ and $g_2 = 2$. In this case, only the pair of inner edge channels is backscattered by the local action of the tip, while the outer edge either flows far from the constriction (under the lower gate) or has no counterpart for the backscattering process to occur (upper gate). In this case, the conductance remains G = 2e2/h even when the tip completely pinches off the constriction region. For the mirrored gate configuration in Fig. 3(c) with g1 = 2 and g2 = 0, we obtained similar SGM images. We also studied the configuration depicted in Fig. 3(d) with identical filling factors g1 = g2 = 2 under the split-gates. This situation is fundamentally different from the situations in Figs. 3(b) and (c), because here no unpaired edge channel is flowing through the QPC. The resulting SGM image, however, is similar to those shown in Figs. 3(b) and (c). These results clearly show that the lower bound for the conductance is determined by the number of paired edge channels which can be backscattered. We have obtained very similar results for other bulk 2DES filling factors ($\nu = 2$, 2 spin-resolved edge channels; and $\nu = 6$, 3 spin-degenerate edge channels), which underlines the general validity of our findings to edge channels in the QH regime.

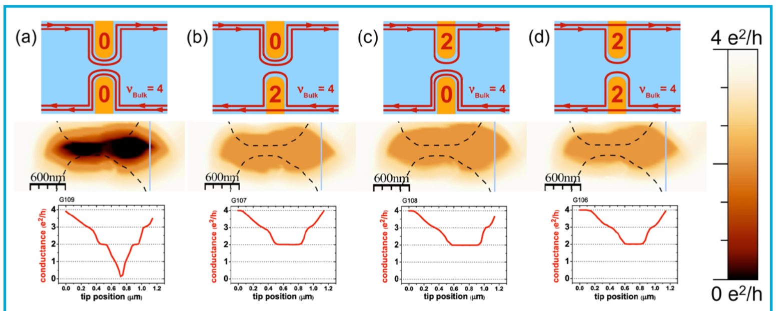

Fig. 3
QPC conductance G as a function of the position of the biased SGM tip. The (bulk) 2DES filling factor is set to $\nu = 4$ (two spin-degenerate edge channels) while the QPC gates partially or completely deplete the 2DES underneath. In (a) gate-region filling factors $g_1 = g_2 = 0$, in (b) $g_1 = 0$, $g_2 = 2$, in (c) $g_1 = 2$, $g_2 = 0$, and in (d) $g_1 = g_2 = 2$. The top row shows sketches of the edge channel trajectories, the center row the SGM conductance images, and the lower row cross sections through the images along the vertical lines drawn in the images. The QPC outline as measured by AFM is indicated by the dashed lines. The color scale of all images ranges from $G = 4e^2/h$ to $0e^2/h$.

In conclusion, we have demonstrated a new method for the control of the trajectories of individual edge channels by the tip of the SGM. Our results can represent a crucial step for the implementation of multi-edge beam mixers and interferometers. We are now working on more refined device geometries to exploit this possibility for a control of the interaction of edge channels in QPC devices in the QH regime.

References

[1] Y. Ji, Y. Chung, D. Sprinzak, M. Heiblum, D. Mahalu, H. Shtrikman, Nature 422 (2003) 415.
[2] I. Neder, N. Ofek, Y. Chung, M. Heiblum, D. Mahalu, V. Umansky, Nature 448 (2007) 333.
[3] V. Giovannetti, F. Taddei, D. Frustaglia, R. Fazio, Phys. Rev. B 77 (2008) 155320.
[4] S. Roddaro, V. Pellegrini, F. Beltram, G. Biasiol, L. Sorba, R. Raimondi, G. Vignale, Phys. Rev. Lett. 90 (2003) 046805.
[5] S. Roddaro, V. Pellegrini, F. Beltram, G. Biasiol, L. Sorba, Phys. Rev. Lett. 93 (2004) 046801.
[6] S. Roddaro, V. Pellegrini, F. Beltram, L.N. Pfeiffer, K. W. West, Phys. Rev. Lett. 95 (2005) 156804.
[7] S. Roddaro, N. Paradiso, V. Pellegrini, G. Biasiol, L. Sorba, F. Beltram, Phys. Rev. Lett. 103 (2009) 016802.
[8] M.A. Topinka, B.J. LeRoy, S.E.J. Shaw, E.J. Heller, R.M. Westervelt, K.D. Maranowski, A.C. Gossard, Science 289 (2000) 2323.
[9] M.A. Topinka, B.J. LeRoy, R.M. Westervelt, S.E.J. Shaw, R. Fleischmann, E.J. Heller, K.D. Maranowski, A.C. Gossard, Nature 410 (2001) 183.